Anthropogenic contributions to the 2021 Pacific Northwest heatwave

Emily Bercos-Hickey[1], Travis A. O'Brien[2,1], Michael F. Wehner[1], Likun Zhang[3,1], Christina M. Patricola[4,1], Huanping Huang[1], Mark D. Risser[1]

[1]Climate and Ecosystem Sciences Division, Lawrence Berkeley National Laboratory, Berkeley, California, USA
[2]Department of Earth and Atmospheric Sciences, Indiana University, Bloomington, Indiana, USA
[3]Department of Statistics, University of Missouri, Columbia, Missouri, USA
[4]Department of Geological and Atmospheric Sciences, Iowa State University, Ames, Iowa, USA

Key Points:

- The Pacific Northwest heatwave was a compound event involving a blocking pattern, atmospheric river, drought conditions, and climate change.
- Statistical and global climate models fail to inform about human influence on the Pacific Northwest heatwave due to the event's uniqueness.
- Hindcast attribution methods can provide limited and conditional information about the human influence on the Pacific Northwest heatwave.

Corresponding author: Emily Bercos-Hickey, ebercoshickey@lbl.gov

Abstract

Daily maximum temperatures during the 2021 heatwave in the Pacific Northwest United States and Canada shattered century old records. Multiple causal factors, including anthropogenic climate change, contributed to these high temperatures, challenging traditional methods of attributing human influence. We demonstrate that the observed 2021 daily maximum temperatures are far above the bounds of Generalized Extreme Value distributions fitted from historical data. Hence, confidence in Granger causal inference statements about the human influence on this heatwave is low. Alternatively, we present a more conditional hindcast attribution study using two regional models. We performed ensembles of simulations of the heatwave to investigate how the event would have changed if it had occurred without anthropogenic climate change and with future warming. We found that human activities caused a 1°C increase in heatwave temperatures. Future warming would lead to a 5°C increase in heatwave temperature by the end of the 21^{st} century.

Plain Language Summary

While it is clear that global warming causes heatwaves to be warmer, the unique meteorological conditions behind the 2021 Pacific Northwest heatwave tax our ability to make quantitative estimates of the human contribution. We discuss why there is low confidence in traditional estimates of the human contribution to this heatwave's temperatures and present an alternative, albeit more highly constrained estimate that human activities caused a 1°C increase in the observed daily maximum temperatures. Additional future warming would lead to a 5°C increase in the heatwave by the end of the 21^{st} century.

1 Introduction

On June 26–29, 2021, an unprecedented heatwave affected the Pacific Northwest (PNW) of the United States and western Canada. Temperature records were shattered, with all-time highs of 116°F (47°C) in Portland, Oregon, 108°F (42°C) in Seattle, Washington, and 121°F (49°C) in Lytton, British Columbia (Di Liberto, 2021). Heatwaves, characterized by prolonged periods of excessive heat, can have dangerous impacts on human health, infrastructure, and the environment (McEvoy et al., 2009; Perkins-Kirkpatrick & Alexander, 2013; Campbell et al., 2018; Ruffault et al., 2020), and the PNW heatwave was no exception. Over 500 deaths were attributed to the heatwave (Popovich & Choi-Schagrin, 2021), and the environment and infrastructure throughout the affected region were strained and damaged, with crops ruined and roads buckled due to the excessively hot temperatures (Baker & Sergio, 2021). The devastating and large-scale impacts of the PNW heatwave were exacerbated by the lack of adaptability of a region unaccustomed to such extreme high temperatures, with the observational record suggesting that this was a highly anomalous event (Figure 1).

The meteorological conditions of the PNW heatwave were similar to previous deadly heatwaves in Europe and Russia (Black et al., 2004; Dole et al., 2011). These events are associated with atmospheric blocking patterns, which are known to cause extreme heatwaves (Miralles et al., 2014; Horton et al., 2015; Schaller et al., 2018) and are characterized by a persistent, quasi-stationary, and often anticyclonic obstruction of the usual zonal flow (Rex, 1950; Sumner, 1954; Woollings et al., 2018). During the PNW heatwave, the high pressure of an omega block was centered over Washington and British Columbia (Figure S1) leading to subsidence and a multi-day period of hot, dry weather throughout the region (Neal et al., 2022). Additionally, an anomalous warm-season atmospheric river (AR) made landfall over the Alaska panhandle in late June and injected a large amount of moisture into western Canada and the PNW. The accumulation of water vapor under the high pressure of the atmospheric blocking pattern may have formed a positive

feedback loop that further enhanced the heatwave (Lin et al., 2022; Mo et al., 2022). These two weather patterns were also superimposed on dry soil conditions, as 50% of Washington state and 70% of Oregon were in severe drought conditions in June 2021 (droughtmonitor.uni.edu).

The unprecedented nature of the PNW heatwave is also consistent with expectations from global warming (Perkins-Kirkpatrick & Gibson, 2017). Heatwaves have increased since the 1950s (Perkins, 2015), and this observed increase in the frequency, intensity, and duration of heatwaves has been attributed to anthropogenic climate change (Meehl & Tebaldi, 2004; Diffenbaugh & Ashfaq, 2010; Perkins et al., 2012; Wuebbles et al., 2014; Min et al., 2013; Wehner et al., 2018). The Intergovernmental Panel on Climate Change (IPCC) Sixth Assessment Report found that many heatwaves around the world could be attributed to human influence (Seneviratne et al., 2021). Future warming will further increase the frequency, intensity, and duration of heat extremes (Vogel et al., 2020), with the potential for temperatures to often reach dangerous levels for human health and agriculture (Sun et al., 2019).

The World Weather Attribution initiative (WWA, https://www.worldweatherattribution.org/) performed analyses of the PNW heatwave within weeks of the event and made three rapid attribution statements, which were later published (Philip et al., 2021). First, the observed temperatures recorded were "virtually impossible" without anthropogenic climate change. Second, after estimating that the observed temperatures had a return period of approximately 1000 years, such annual maximum daily maximum temperatures (TXx) "would have been at least 150 times rarer without human-induced climate change". Third, the heatwave was about 2°C warmer than it would have been without climate change based on the change in 1000 year return values of TXx.

In this study, our objective is to revisit these rapid attribution statements and to advance our understanding of how climate change affected the PNW heatwave. In section 2, we discuss the limitations of statistical models to estimate the rarity of the PNW heatwave. In section 3, we describe our experimental design of dynamical model simulations of the PNW heatwave under past, present, and future climate conditions using two regional climate models. In section 4, we discuss the resulting temperature changes from these simulations. Finally, we present our conclusions in section 5.

2 Statistical modeling

Figure 1a shows maximum daily maximum temperatures between June 25 and July 4, 2021 from the Global Historical Climatology Network (GHCN) station data. Figure 1a reveals that most stations in this region had values greater than 45°C. Figure 1b compares the summertime (June/July/August, JJA) TXx from all of the US stations within the WWA region (45°N–49°N, 123°W–119°W) over 1920-2020 to those from June 25 to July 4, 2021. Figure 1c shows JJA TXx averaged over all of the US stations in this region for each year. From Figures 1b,c, it is clear that the PNW heatwave was an outlier event compared to previous summertime maximum temperatures and will challenge statistical modeling.

Philip et al. (2021) found that the 2021 spatially averaged temperatures from the ERA5 reanalysis (Hersbach et al., 2020) exceeded the upper bound of an out of sample non-stationary generalized extreme value (GEV) distribution fit to data from 1950 to 2020. They then included the 2021 values, estimating that the current return period of the PNW heatwave was about 1000 years. Comparing this return period to that obtained under preindustrial temperatures, they concluded that the probability of the PNW heatwave was increased by a factor of 390. Further analysis of climate model simulations and their expert judgement caused them to conclude that the probability of the observed temperature was increased by *at least* 150 as their final synthesis attribution statement.

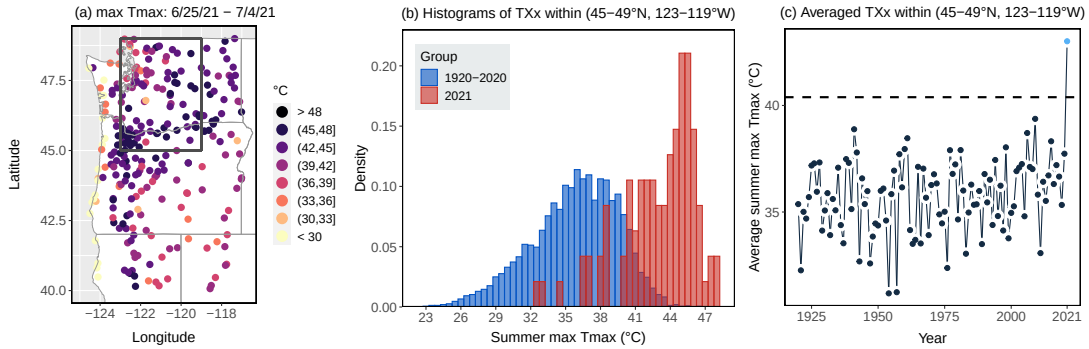

Figure 1. Observational station data from the Global Historical Climatology Network (GHCN) of (a) the maximum daily maximum temperature between June 25 and July 4, (b) histograms of the summertime (June/July/August, JJA) maximum daily maximum temperature (i.e., JJA TXx) from the US stations within the WWA region (45°N–49°N, 123°W–119°W), as defined by Philip et al. (2021), in 1920-2020 and in 2021 and (c) the average JJA TXx by year from the US stations within the same region. The dashed line is the Bayesian expectation of the upper bound on daily maximum temperature averaged across the US stations within the WWA region.

We repeat this non-stationary GEV analysis on individual station data from 1950-2020 instead of averaging over the WWA study region. In each single-station analysis, we use a GEV distribution with a location parameter linearly dependent on a sum-total forcing variable for five well-mixed greenhouse gases to accommodate non-stationarity (e.g. Risser et al. (2022)), which imposes a non-linear time trend in the GEV model. Details of the GEV analysis are discussed in Supplemental Section 1.

Figure 2a shows the Bayesian expectation of the upper bound for daily maximum temperatures for the 1950-2020 GHCN station data. Stations where the observed 2021 values exceed the expectation of the upper bound ('+') reveal that most of the heatwave's maximum temperatures are outside of the range of the GEV model. Figure 2b shows the 2021 out of sample return times for the GHCN stations, where many stations realized return times in excess of 2000 years during the 2021 PNW heatwave. The probability of 2021 temperatures exceeding this GEV upper bound (Figure 2c) further illustrates that the out of sample GEV fails to describe the 2021 PNW heatwave. Including the 2021 temperatures in the GEV fitting procedure extends the upper bounds to include these values in the distribution, but the distributions are a poor fit to the rest of the data. Using a χ^2 goodness-of-fit test, the p-values calculated without 2021 values are generally greater than 0.2, demonstrating strong evidence of an underlying GEV distribution. However, the p-values calculated when 2021 temperatures are included are less than 0.05, indicating that the distribution is significantly different from GEV. Figure 1b, constructed by binning all GHCN station data from 1920-2020 (blue) and 2021 (red), further suggests that the temperatures of the 2021 heatwave are drawn from different distributions than previous years that is not accounted for by the time-dependent greenhouse gas covariate. The above evidence suggest that the critical GEV assumption of independent and identically distributed (i.i.d.) data is violated when 2021 temperatures are included.

Given that an in-sample GEV distribution is a poor fit to the GHCN data and that the combined effects of the atmospheric blocking pattern and anomalous AR were likely unique, we conclude that there should be little confidence in attribution statements based on in-sample GEV formulations. Philip et al. (2021) argued that the temperatures reached

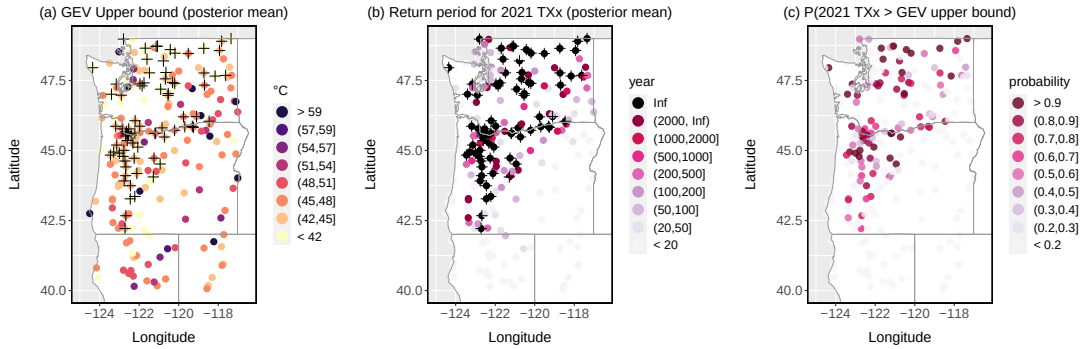

Figure 2. Results from fitting the non-stationary GEV distribution to station data from 1950 to 2020: (a) Bayesian expectation (posterior mean) for the GEV distributional upper bound; (b) Bayesian expectation for the return periods of 2021 JJA TXx (calculated using the fitted non-stationary GEV distribution). In both panels, '+' signifies that the 2021 JJA TXx exceeded the Bayesian expectation of the GEV distributional upper bound, which leads to infinite return periods in (b); (c) The overall probability of 2021 TXx exceeding the GEV upper bound given the observations.

during the PNW heatwave were "virtually impossible" without climate change. However, this is not supported from a purely Granger causal inference perspective (Ebert-Uphoff & Deng, 2012; Hannart et al., 2016) due to the failure of the GEV methodology. Our statistical analysis supports an attribution statement that these temperatures were virtually impossible under any previously experienced meteorological conditions, with or without global warming. Pearl causal inference statements (Pearl, 2009) about the change in magnitude of the PNW heatwave from global warming, assuming a fixed but unspecified return time, can be informed by climate models as discussed in the next section.

3 Dynamical Models and Experimental Design

From section 2, the PNW heatwave of 2021 was an extreme outlier event. Traditionally, Pearl causal inference attribution statements are made with long simulations of global climate models, usually in pairs forced with both anthropogenic and natural forcing factors (Stott et al., 2016). However, another more conditional form of Pearl causal inference attribution statements can be formulated with the hindcast attribution (Wehner et al., 2019) or pseudo-global warming (PGW) method (Schär et al., 1996; Patricola & Wehner, 2018; Bercos-Hickey & Patricola, 2021; Bercos-Hickey et al., 2021; Patricola et al., 2022). In this approach, ensembles of regional climate model simulations are performed with historical initial and boundary conditions and are then compared with simulations performed with counterfactual initial and boundary conditions that have been adjusted by a climate change difference, or delta, that takes into account the thermodynamic component of anthropogenic climate change. While no attribution statement can be made about the human-induced change in probability of the event, quantitative attribution statements about the human-induced change in the magnitude of the event can be made with this more restricted approach.

In this study, the Weather Research and Forecasting (WRF) model (Skamarock et al., 2008) version 3.8.1 was used to perform hindcast simulations of the PNW heatwave. To understand the impacts of model structural uncertainty, we performed a similar suite of simulations using the International Centre for Theoretical Physics Regional

Climate Model (RegCM) version 4.9.5 (Giorgi et al., 2012). The WRF hindcast simulations were initialized on June 24, 2021 0000 UTC and ran continuously through July 4, 2021 with initial and boundary conditions from the 32 km resolution National Centers for Environmental Prediction (NCEP) North American Regional Reanalysis (NARR). Further details of the WRF simulations are discussed in Supplemental Section 2. The RegCM hindcast simulations were initialized on June 22, 2021 0000 UTC and ran continuously through July 02, 2021 with initial and boundary conditions from the Global Forecast System (GFS) version 4 0.5-degree analysis. Further details of the RegCM simulations are discussed in Supplemental Section 3. Ten-member ensembles were performed for each model configuration and the effects of horizontal resolution were explored by configuring the models with grids of 18 km and 50 km spacings over the chosen domains (Figure S2).

To establish the validity of the heatwave simulations, we compare the WRF and RegCM hindcasts with observational and reanalysis data. As shown in Supplemental Section 4, the WRF and RegCM hindcasts accurately capture the key features of the PNW heatwave. The hindcasts of the heatwave event were best represented at 18 km (Supplemental Section 4), and thus for the remainder of the analysis we use the 18 km resolution simulations.

In addition to the hindcast simulations, three ten-member ensembles under counterfactual conditions were performed using the PGW method to understand the effects of global warming on the PNW heatwave. The cooler "world that might have been" without the current amount of anthropogenic climate change permits attribution statements about the observed magnitude of the event. Two warmer "worlds that might be" simulations were performed with mid- and late-21st century climate conditions under the Shared Socioeconomic Pathway 585 (SSP585) emissions scenario (O'Neill et al., 2016) to further elucidate the effect of global warming on the event. For the "world that might have been", the deltas were calculated using the difference between historical and naturally forced (*hist-nat*) simulations from the multi-model average of the Coupled Model Intercomparison Project Phase 6 (CMIP6) (Danabasoglu, 2019) data (see Table S1). Thus the effects of anthropogenic forcing are removed but the natural solar and volcanic forcing effects are retained. The "world that might be" deltas were calculated using the difference between the historical and mid- and late-21st century future SSP585 simulations from the CMIP6 multi-model average. Additional details on the PGW experiments are discussed in Supplemental Section 5. Lastly, to examine the effects of climate change on soil moisture-temperature feedbacks, hist-nat, mid-, and late-21st century experiments were conducted with the 18 km WRF model by additionally altering soil moisture. A summary of all model experiments is shown in Table S2.

In the following section, our analyses utilize spatial averages over the region 45°N-52°N and 124°W-119°W (Figure S2). Because WRF and RegCM were run at finer resolution than the CMIP-class models in Philip et al. (2021), we extended the region of interest to the west to be closer to the coast than the WWA region.

4 Changes in PNW heatwave temperature

The effects of the current amount of climate change on the PNW heatwave are assessed by comparing the WRF and RegCM simulations in the historical and hist-nat climates. Figure 3 shows the June 25-July 1, 2021 time series of (a) the GHCN, NARR, GFS, WRF, and RegCM daily maximum temperature and (b) the WRF and RegCM temperature differences between the climate scenarios and the historical. Contours of the maximum temperature on June 28, the hottest day of the GHCN station observations (Figure 3a), are shown for the (c)(f) historical, (d)(g) historical minus hist-nat, and (e)(h) late-century minus historical simulations from the 18 km (c)-(e) WRF and (f)-(h) RegCM. From Figure 3d, the WRF model clearly exhibits warming from the hist-

nat to the historical climate except for some cooling at the Oregon coast. From Figure 3g, the RegCM model exhibits a more hetereogeneous warming and the cooling is shifted northward to the coast of British Columbia. In our analysis region (Figures 3c,f black box), the ensemble average increase in the daily maximum two-meter temperature on June 28 is 0.95±0.22°C for WRF and 0.66±0.05°C for RegCM from the hist-nat to the historical, where the uncertainty bounds are calculated from the standard error. Over the four-day period June 27-30, during which multiple temperature records were broken, the average increase in daily maximum two-meter temperature is 0.98±0.40°C for WRF and 0.78±0.07°C for RegCM from the hist-nat to the historical. The blue lines in Figure 3b reveal that the attributable warming in the WRF model averaged over the region of interest (about 1°C) does not change much during the heatwave event. The RegCM, which here differs from the WRF model in that soil moisture was not altered in the hist-nat simulations, exhibits a decrease in attributable warming until June 28 and then an increase until July 1.

Figure 3e shows that the WRF simulated heatwave is warmer over the entire domain under late-century conditions when compared to the historical simulations. Similar warming is also seen in the WRF simulations under mid-century conditions (not shown). In contrast, Figure 3h shows that while the RegCM model warms over the majority of the region under late-century conditions, cooling is simulated along the coast of southern Oregon and northern California. This coastal cooling in the RegCM late-century simulations is likely due to a complicated interaction between changes in onshore winds and a warmed ocean and is influenced by the choice of boundary layer parameterization scheme. In our analysis region (Figures 3c,f black box), the average increase in the daily maximum two-meter temperature on June 28 is 1.55±0.29°C for WRF from the historical to the mid-century, and is 4.68±0.26°C for WRF and 4.57±0.04°C for RegCM from the historical to the late-century. During the peak days of the heatwave, the June 27-30 average increase in maximum daily two-meter temperature is 1.71±0.39°C for WRF from the historical to the mid-century, and is 5.41±0.41°C for WRF and 5.20±0.06°C for RegCM from the historical to the late-century.

The red lines in Figure 3b compare the regionally averaged temperature change between the present and late-century under SSP585 forcing conditions. The orange line shows a similar result for the WRF model under mid-century SSP585 forcing conditions. In these warmer simulations, the anthropogenic warming of the PNW heatwave gradually reduces until the hottest days are reached, June 29, 2021. Afterwards, the anthropogenic warming increases as the heatwave evolves for both models, lengthening the duration of the heatwave in both the WRF and RegCM simulations. This behavior is also exhibited in the RegCM historical compared to hist-nat simulations (blue dashed line), but is not for WRF, where the regionally averaged anthropogenic warming is relatively constant over the entire duration of the simulation.

To examine the effects of soil moisture-temperature feedback on the PNW heatwave, we performed WRF experiments with and without the soil moisture delta. Inclusion of the soil moisture delta causes warmer climates to have drier soil and cooler climates to have wetter soil. Figure 4 shows the June 28, 2021 ensemble-averaged maximum two-meter temperature from the 18 km WRF (a) hist-nat, (b) mid-century, and (c) late-century experiments with the soil moisture delta minus the experiments without the soil moisture delta. Panel (d) shows the June 25-July 1 time series of the daily maximum temperature in the soil moisture minus no soil moisture experiments. From Figure 4a, the heatwave in the hist-nat climate is cooler across most of the region when the soil moisture delta is included, reflecting an increase in evapotranspiration cooling. In our analysis region (Figures 3c,f black box), the average daily maximum two-meter temperature in Figure 4a is 0.10±0.21°C cooler in the hist-nat experiment with the soil moisture delta than it is without. Figures 4b,c indicate that the heatwave in the mid- and late-century climates is warmer across almost all of the region when the soil mois-

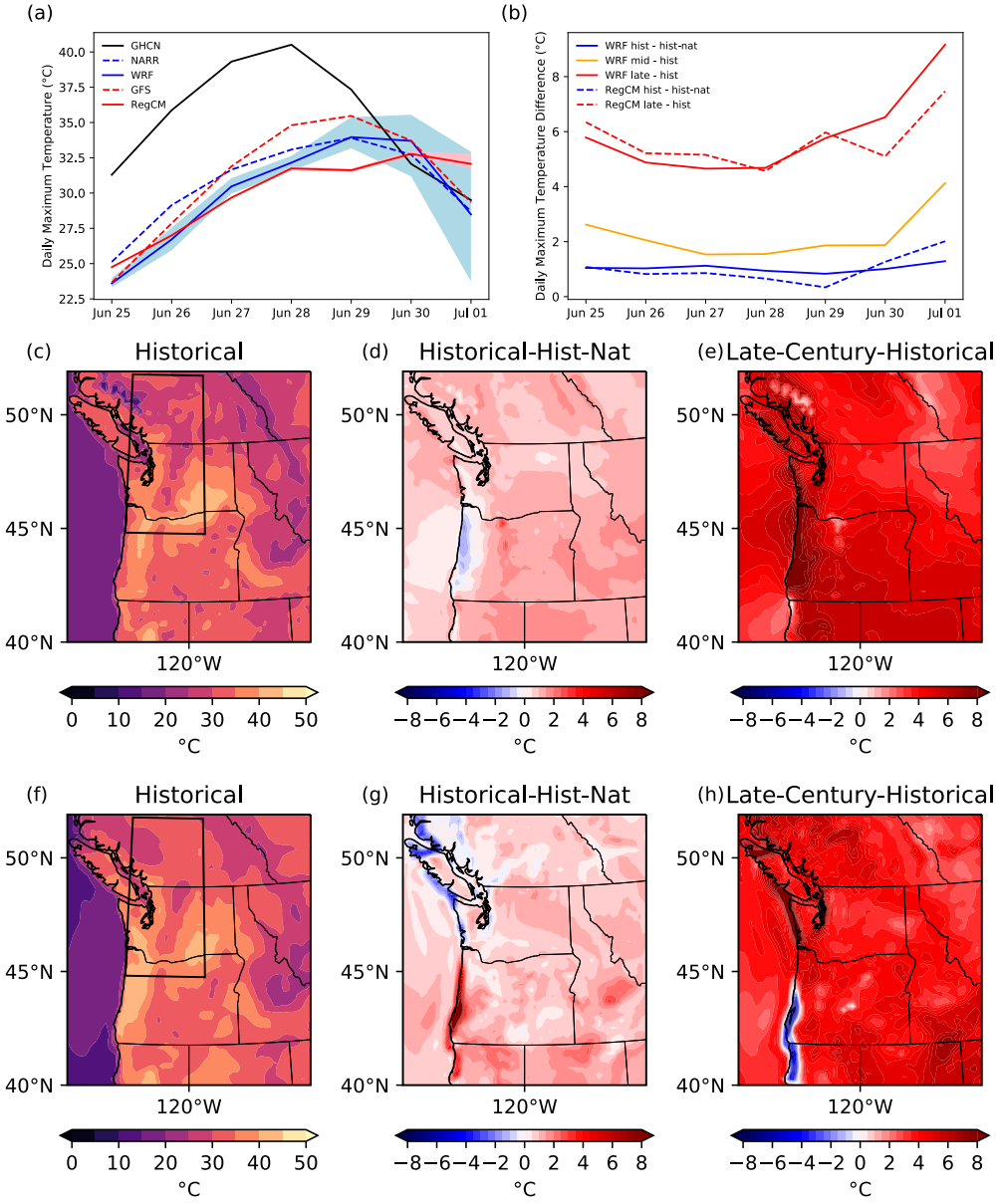

Figure 3. June 25-July 1, 2021 daily maximum temperature (a) from the GHCN, NARR, GFS, and the WRF and RegCM historical 18 km ensembles, and daily maximum temperature difference (b) between the WRF and RegCM historical and hist-nat, mid-century (WRF only), and late-century ensembles averaged over the region 45°N-52°N and 124°W-119°W. The shading in panel (a) shows the range of values over the WRF and RegCM 10-member ensembles. Ensemble-averaged daily maximum 2 m temperature (°C) on June 28 of the (c)(f) historical, (d)(g) historical minus hist-nat, and (e)(h) late-century minus historical simulations from the 18 km (c)-(e) WRF with the soil moisture delta and (f)-(h) RegCM. Black boxes in panels (c) and (f) are the regions used for spatial averaging, also shown in Figure S2.

ture delta is included, reflecting a decrease in evapotranspiration cooling due to less available soil moisture. The average daily maximum two-meter temperature in Figures 4b,c is 0.78±0.34°C and 0.90±0.28°C warmer in the mid- and late-century experiments with the soil moisture delta, respectively.

The blue line in Figure 4d reveals that the effects of soil moisture on the hist-nat simulations remains relatively constant throughout the duration of the heatwave. In contrast, the future climate simulations (Figure 4d orange and red lines) exhibit a temporally dependent enhancement of the effects of the soil moisture delta as the heatwave progresses. Roughly following the simulated temperature itself (Figure 3a), the effect of decreased soil moisture peaks at about 1.0 °C and 1.2°C warmer in the mid- and late-century experiments, respectively.

5 Conclusions

The 2021 Pacific Northwest (PNW) heatwave was a rare and unprecedented compound weather event. An unusual summertime atmospheric river interacted with an omega block pattern and preexisting dry soil conditions to shatter century-old temperature records by several degrees Centigrade. While there is little doubt that anthropogenic global warming contributed to the probability and magnitude of the extreme temperatures, the uniqueness of the event precludes quantifying this influence by traditional event attribution methods. In section 2, we demonstrated that out of sample fitted non-stationary Generalized Extreme Value (GEV) distributions fail to contain many of the observed 2021 observations within the uncertainty estimates of their upper bounds. While including the 2021 temperatures in the GEV fitting procedure extends the upper bounds to include these values in the distribution, these distributions are a poor fit to the rest of the data. The underlying reason for this failure of traditional statistical methods is that the uniqueness of the 2021 PNW heatwave violates the i.i.d. assumption of GEV theory. We therefore conclude that estimates of the PNW heatwave return times are not accurate and that confidence in GEV-based estimates of the human influence on the change in the probability of the observed extreme temperatures should be low. We further conclude that quantitative changes in event magnitude and frequency from CMIP-class models (Wehner et al., 2020, 2018; Philip et al., 2021) are made with low confidence as it is not clear that global climate models can adequately simulate the relevant meteorological phenomena of the PNW heatwave (van Oldenborgh et al., 2021, 2022).

In sections 3,4, we present an alternative but more limited attribution of the anthropogenic changes to the PNW heatwave using ensembles of simulations from the regional models WRF and RegCM, where the pseudo-global warming (PGW) method was used to examine the effects of removing anthropogenic warming and additional future warming. We find that the historical model simulations are in agreement with their initial and boundary condition datasets, but that the observed and simulated gridded products are cooler than station observations during the hot portion of the event. Comparison of the historical heatwave with a counterfactual heatwave in a world without human-induced warming indicates that the anthropogenic temperature increase is about 1°C and relatively constant over the course of the event. In contrast, the heatwave in an SSP585 world with significant future warming would be 5°C warmer, and the anthropogenic influence extends the peak of the heatwave, indicating a future increase in heatwave duration.

These anthropogenic increases in extreme temperatures during the PNW heatwave are less than previous estimates (Philip et al., 2021). One possible reason for this is that severe drought conditions were being experienced in June 2021 in much of the southern portion of our analysis region, reducing the evapotranspiration cooling in our cooler counterfactual "world that might have been". In section 4, we examined the effects of soil moisture in the PGW experiments and found that, at current levels of global warming,

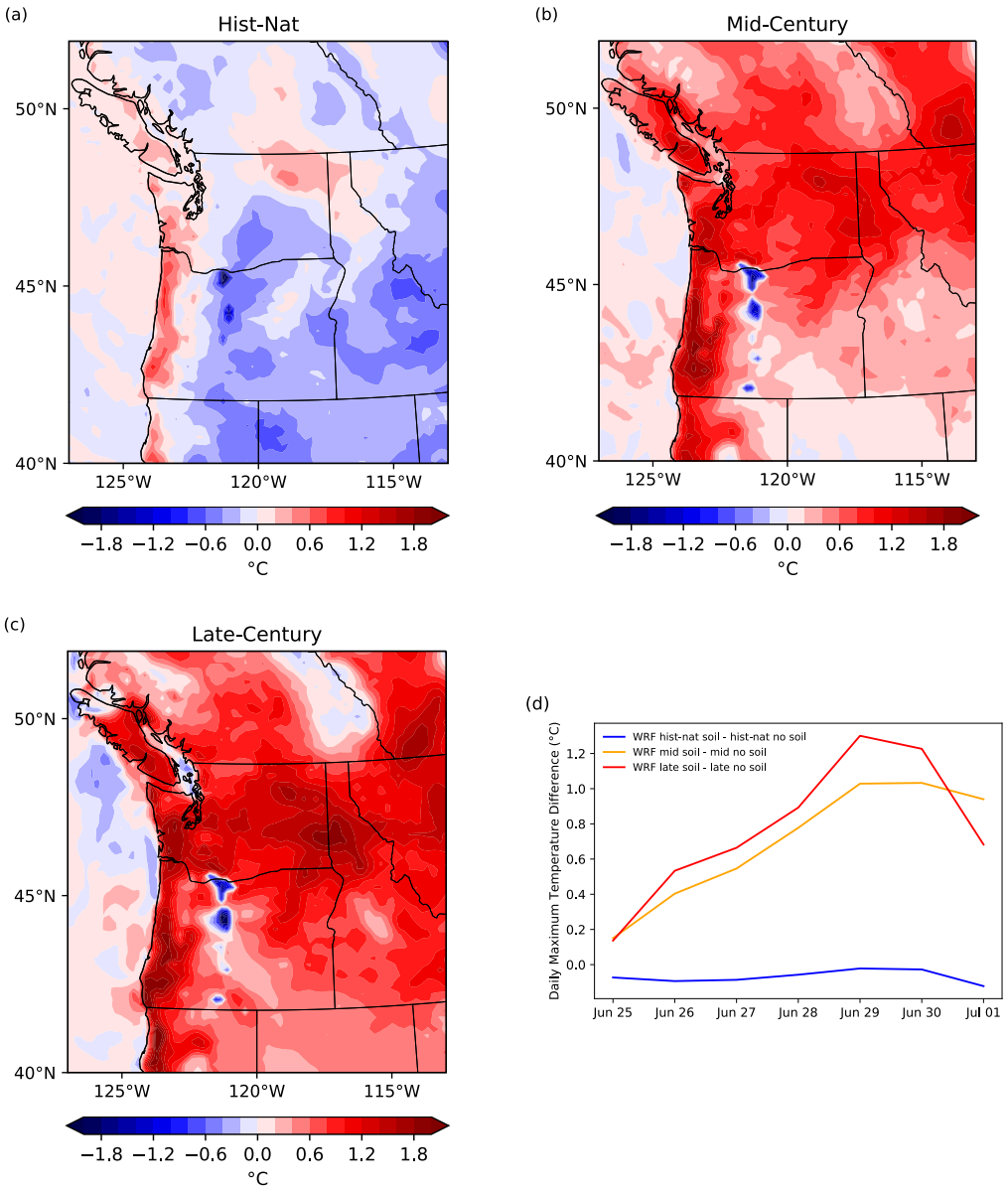

Figure 4. Ensemble-averaged daily maximum 2 m temperature (°C) on June 28, 2021 from the 18 km WRF (a) hist-nat, (b) mid-century, and (c) late-century experiments with the soil moisture delta minus the experiments without the soil moisture delta. The June 25-July 1, 2021 daily maximum temperature difference between the experiments with and without the soil moisture delta averaged over the region 45°N-52°N and 124°W-119°W (d).

this cooling is altered by only about 0.10°C. As precursor soil conditions from the drought are drier than the average conditions used in traditional CMIP-class heatwave attribution statements, this is not unexpected. Even in much warmer late-century conditions, the maximum soil moisture-temperature feedback is 1.2°C out of over 6°C averaged over our analysis region. While it may be that the amplification of the anthropogenic temperature change during heatwaves (Seneviratne et al., 2021) is diminished by pre-existing drought conditions, this is not the case in much warmer future simulations. Clearly, our understanding of all the physical mechanisms behind this extreme heatwave and their anthropogenic changes is limited (van Oldenborgh et al., 2022) and our traditional attribution tools fail for this and other extreme outlier events. However, there may be opportunities to remedy this by examining the large coupled and uncoupled model ensembles (Kay et al., 2015; Stone et al., 2019). Presently, however, we do not know with confidence whether the 2021 PNW heatwave and the associated weather patterns will remain an outlier event or is a harbinger of things to come.

Open Research

The WRF and RegCM simulation data used for the pseudo-global warming analysis in the study are available at https://portal.nersc.gov/cascade/PNW_Heatwave. CMIP6 data is available through Danabasoglu (2019).

Acknowledgments

This material is based upon work supported by the U.S. Department of Energy, Office of Science, Office of Biological and Environmental Research, Climate and Environmental Sciences Division, Regional & Global Model Analysis Program, under Award Number DE-AC02-05CH11231. This research used resources of the National Energy Research Scientific Computing Center (NERSC), a DOE Office of Science User Facility supported by the Office of Science of the U.S. DOE under Contract No. DE-AC02-05CH11231. We acknowledge the World Climate Research Programme, which, through its Working Group on Coupled Modelling, coordinated and promoted CMIP6. We thank the climate modeling groups for producing and making available their model output, the Earth System Grid Federation (ESGF) for archiving the data and providing access, and the multiple funding agencies who support CMIP6 and ESGF. This project was also partially supported by the Environmental Resilience Institute, funded by Indiana University's Prepared for Environmental Change Grand Challenge initiative.

References

Baker, M., & Sergio, O. (2021). The pacific northwest, built for mild summers, is scorching yet again. *New York Times*.

Bercos-Hickey, E., & Patricola, C. M. (2021). Anthropogenic influences on the african easterly jet–african easterly wave system. *Climate Dynamics*. doi: 10.1007/s00382-021-05838-1

Bercos-Hickey, E., Patricola, C. M., & Gallus, W. A. (2021). Anthropogenic Influences on Tornadic Storms. *Journal of Climate*, *34*(22), 8989–9006. Retrieved from `https://journals.ametsoc.org/view/journals/clim/aop/JCLI-D-20-0901.1/JCLI-D-20-0901.1.xml` doi: 10.1175/JCLI-D-20-0901.1

Berner, J., Ha, S.-Y., Hacker, J. P., Fournier, A., & Snyder, C. (2011). Model uncertainty in a mesoscale ensemble prediction system: Stochastic versus multiphysics representations. *Monthly Weather Review*, *139*(6), 1972-1995.

Black, E., Blackburn, M., Harrison, G., Hoskins, B., & Methven, J. (2004). Factors contributing to the summer 2003 european heatwave. *Weather*, *59*(8), 217-223. doi: https://doi.org/10.1256/wea.74.04

Campbell, S., Remenyi, T. A., White, C. J., & Johnston, F. H. (2018). Heatwave

and health impact research: A global review. *Health & Place*, *53*, 210-218.

Chen, F., & Dudhia, J. (2001). Coupling an advanced land surface–hydrology model with the penn state–ncar mm5 modeling system. part i: Model implementation and sensitivity. *Monthly Weather Review*, *129*(4), 569-585.

Danabasoglu, G. (2019). *NCAR CESM2 model output prepared for CMIP6 CMIP.* Earth System Grid Federation. Retrieved from `https://doi.org/10.22033/ESGF/CMIP6.2185` doi: 10.22033/ESGF/CMIP6.2185

Dickinson, R. E., Henderson-Sellers, A., Kennedy, P. J., & Wilson, M. F. (1993). Biosphere atmosphere transfer scheme (BATS) version 1e as coupled for Community Climate Model. *NCAR Tech. Note NCAR/TN-378+SR*(August), 77. doi: 10.1029/2009JD012049

Diffenbaugh, N. S., & Ashfaq, M. (2010). Intensification of hot extremes in the united states. *Geophysical Research Letters*, *37*(15). doi: https://doi.org/10.1029/2010GL043888

Di Liberto, T. (2021). Astounding heat obliterates all-time records across the pacific northwest and western canada in june 2021. *National Oceanic and Atmospheric Administration*. Retrieved from `https://www.climate.gov/news-features/event-tracker/astounding-heat-obliterates-all-time-records-across-pacific-northwest`

Dole, R., Hoerling, M., Perlwitz, J., Eischeid, J., Pegion, P., Zhang, T., ... Murray, D. (2011). Was there a basis for anticipating the 2010 russian heat wave? *Geophysical Research Letters*, *38*(6). doi: https://doi.org/10.1029/2010GL046582

Ebert-Uphoff, I., & Deng, Y. (2012). Causal discovery for climate research using graphical models. *Journal of Climate*, *25*(17), 5648 - 5665. Retrieved from `https://journals.ametsoc.org/view/journals/clim/25/17/jcli-d-11-00387.1.xml` doi: 10.1175/JCLI-D-11-00387.1

Emanuel, K. A. (1991, nov). A Scheme for Representing Cumulus Convection in Large-Scale Models. *Journal of the Atmospheric Sciences*, *48*(21), 2313–2329. Retrieved from `http://journals.ametsoc.org/doi/10.1175/1520-0469(1991)048%3C2313:ASFRCC%3E2.0.CO;2` doi: 10.1175/1520-0469(1991)048⟨2313:ASFRCC⟩2.0.CO;2

Emanuel, K. A., & Živković-Rothman, M. (1999, jun). Development and Evaluation of a Convection Scheme for Use in Climate Models. *Journal of the Atmospheric Sciences*, *56*(11), 1766–1782. Retrieved from `http://journals.ametsoc.org/doi/10.1175/1520-0469(1999)056%3C1766:DAEOAC%3E2.0.CO;2` doi: 10.1175/1520-0469(1999)056⟨1766:DAEOAC⟩2.0.CO;2

Etminan, M., Myhre, G., Highwood, E., & Shine, K. (2016). Radiative forcing of carbon dioxide, methane, and nitrous oxide: A significant revision of the methane radiative forcing. *Geophysical Research Letters*, *43*(24), 12–614.

Eyring, V., Bony, S., Meehl, G. A., Senior, C. A., Stevens, B., Stouffer, R. J., & Taylor, K. E. (2016). Overview of the coupled model intercomparison project phase 6 (cmip6) experimental design and organization. *Geosci. Model Dev.*, *9*(5), 1937-1958. doi: 10.5194/gmd-9-1937-2016

Giorgi, F., Coppola, E., Solmon, F., Mariotti, L., Sylla, M., Bi, X., ... Brankovic, C. (2012). RegCM4: model description and preliminary tests over multiple CORDEX domains. *Climate Research*, *52*, 7–29. Retrieved from `http://www.int-res.com/abstracts/cr/v52/p7-29/` doi: 10.3354/cr01018

Grell, G. A., & Freitas, S. R. (2014). A scale and aerosol aware stochastic convective parameterization for weather and air quality modeling. *Atmos. Chem. Phys.*, *14*(10), 5233-5250.

Grenier, H., & Bretherton, C. S. (2001). A Moist PBL Parameterization for Large-Scale Models and Its Application to Subtropical Cloud-Topped Marine Boundary Layers. *Monthly Weather Review*, *129*(3), 357–377. Retrieved from `http://dx.doi.org/10.1175/1520-0493(2001)129%3C0357:AMPPFL%3E2.0.CO%5Cn2` doi: 10.1175/1520-0493(2001)129⟨0357:AMPPFL⟩2.0.CO;2

Hannart, A., Pearl, J., Otto, F. E. L., Naveau, P., & Ghil, M. (2016, jan). Causal Counterfactual Theory for the Attribution of Weather and Climate-Related Events. *Bulletin of the American Meteorological Society*, *97*(1), 99–110. Retrieved from `http://journals.ametsoc.org/doi/abs/10.1175/BAMS-D-14-00034.1` doi: 10.1175/BAMS-D-14-00034.1

Hersbach, H., Bell, B., Berrisford, P., Hirahara, S., Horányi, A., Muñoz-Sabater, J., ... others (2020). The era5 global reanalysis. *Quarterly Journal of the Royal Meteorological Society*, *146*(730), 1999–2049.

Hodnebrog, Ø., Etminan, M., Fuglestvedt, J., Marston, G., Myhre, G., Nielsen, C., ... Wallington, T. (2013). Global warming potentials and radiative efficiencies of halocarbons and related compounds: A comprehensive review. *Reviews of Geophysics*, *51*(2), 300–378.

Hong, S.-Y., & Lim, J.-O. J. (2006). The wrf single-moment 6-class microphysics scheme (wsm6). *Journal of the Korean Meteorological Society*, *42*(2), 129-151.

Hong, S.-Y., & Pan, H.-L. (1996). Nonlocal boundary layer vertical diffusion in a medium-range forecast model. *Monthly Weather Review*, *124*(10), 2322-2339.

Horton, D. E., Johnson, N. C., Singh, D., Swain, D. L., Rajaratnam, B., & Diffenbaugh, N. S. (2015). Contribution of changes in atmospheric circulation patterns to extreme temperature trends. *Nature*, *522*(7557), 465-469.

Iacono, M. J., Delamere, J. S., Mlawer, E. J., Shephard, M. W., Clough, S. A., & Collins, W. D. (2008). Radiative forcing by long-lived greenhouse gases: Calculations with the aer radiative transfer models. *Journal of Geophysical Research*, *113*(D13), D13103.

Kay, J. E., Deser, C., Phillips, A., Mai, A., Hannay, C., Strand, G., ... Vertenstein, M. (2015). The Community Earth System Model (CESM) Large Ensemble Project: A Community Resource for Studying Climate Change in the Presence of Internal Climate Variability. *Bulletin of the American Meteorological Society*, *96*(8), 1333–1349. doi: 10.1175/BAMS-D-13-00255.1

Kiehl, J., Hack, J., Bonan, G., Boville, B., Briegleb, B., Williamson, D., & Rasch, P. (1996). *Description of the NCAR Community Climate Model (CCM3)* (Tech. Rep. No. September). doi: 10.5065/D6FF3Q99

Lin, H., Mo, R., & Vitart, F. (2022). The 2021 western north american heatwave and its subseasonal predictions. *Geophysical Research Letters*, e2021GL097036. doi: https://doi.org/10.1029/2021GL097036

McEvoy, D., Ahmed, I., & Mullett, J. (2009). The impact of the 2009 heat wave on melbourne's critical infrastructure. *Local Environment*, *17*(8), 783-796.

Meehl, G. A., & Tebaldi, C. (2004). More intense, more frequent, and longer lasting heat waves in the 21st century. *Science*, *305*(5686), 994 LP - 997.

Meinshausen, M., & Nicholls, Z. R. J. (2018). *Uom-remind-magpie-ssp585-1-2-0: Remind-magpie-ssp585 ghg concentrations.* Earth System Grid Federation. Retrieved from `https://doi.org/10.22033/ESGF/input4MIPs.2349` doi: 10.22033/ESGF/input4MIPs.2349

Meinshausen, M., & Vogel, E. (2016). input4mips.uom.ghgconcentrations.cmip.uom-cmip-1-2-0. *Earth System Grid Federation*. doi: 10.22033/ESGF/input4MIPs.1118

Min, S.-K., Zhang, X., Zwiers, F., Shiogama, H., Tung, Y.-S., & Wehner, M. (2013, jun). Multimodel Detection and Attribution of Extreme Temperature Changes. *Journal of Climate*, *26*(19), 7430–7451. doi: 10.1175/JCLI-D-12-00551.1

Miralles, D. G., Teuling, A. J., van Heerwaarden, C. C., & Vilà-Guerau de Arellano, J. (2014, may). Mega-heatwave temperatures due to combined soil desiccation and atmospheric heat accumulation. *Nature Geoscience*, *7*(5), 345–349. Retrieved from `http://www.nature.com/articles/ngeo2141` doi: 10.1038/ngeo2141

Mo, R., Lin, H., & Vitart, F. (2022). An anomalous atmospheric river linked to the late june 2021 western north america heatwave. *Commun. Earth Environ.*. (in

revision)

Neal, E., Huang, C. S. Y., & Nakamura, N. (2022). The 2021 pacific northwest heat wave and associated blocking: Meteorology and the role of an upstream cyclone as a diabatic source of wave activity. *Geophysical Research Letters*, *49*(8), e2021GL097699. Retrieved from `https://agupubs.onlinelibrary.wiley.com/doi/abs/10.1029/2021GL097699` (e2021GL097699 2021GL097699) doi: https://doi.org/10.1029/2021GL097699

O'Brien, T. A., Chuang, P. Y., Sloan, L. C., Faloona, I. C., & Rossiter, D. L. (2012). Coupling a new turbulence parametrization to RegCM adds realistic stratocumulus clouds. *Geoscientific Model Development*, *5*(4), 989–1008. doi: 10.5194/gmd-5-989-2012

O'Brien, T. A., Sloan, L. C., & Snyder, M. A. (2011, sep). Can ensembles of regional climate model simulations improve results from sensitivity studies? *Climate Dynamics*, *37*(5-6), 1111–1118. Retrieved from `http://link.springer.com/10.1007/s00382-010-0900-5` doi: 10.1007/s00382-010-0900-5

O'Neill, B. C., Tebaldi, C., Van Vuuren, D. P., Eyring, V., Friedlingstein, P., Hurtt, G., ... Sanderson, B. M. (2016). The Scenario Model Intercomparison Project (ScenarioMIP) for CMIP6. *Geoscientific Model Development*, *9*(9), 3461–3482. doi: 10.5194/gmd-9-3461-2016

Patricola, C. M., & Wehner, M. F. (2018). Anthropogenic influences on major tropical cyclone events. *Nature*, *563*(7731), 339-346.

Patricola, C. M., Wehner, M. F., Bercos-Hickey, E., Maciel, F. V., May, C., Mak, M., ... Leal, S. (2022). Future changes in extreme precipitation over the san francisco bay area: Dependence on atmospheric river and extratropical cyclone events. *Weather and Climate Extremes*, *36*, 100440. Retrieved from `https://www.sciencedirect.com/science/article/pii/S2212094722000275` doi: https://doi.org/10.1016/j.wace.2022.100440

Pearl, J. (2009). *Causality*. Cambridge, U. K., Cambridge University Press.

Perkins, S. E. (2015). A review on the scientific understanding of heatwaves—their measurement, driving mechanisms, and changes at the global scale. *Atmospheric Research*, *164-165*, 242-267.

Perkins, S. E., Alexander, L. V., & Nairn, J. R. (2012). Increasing frequency, intensity and duration of observed global heatwaves and warm spells. *Geophysical Research Letters*, *39*(20). doi: https://doi.org/10.1029/2012GL053361

Perkins-Kirkpatrick, S. E., & Alexander, L. V. (2013). On the measurement of heat waves. *Journal of Climate*, *26*(13), 4500-4517.

Perkins-Kirkpatrick, S. E., & Gibson, P. B. (2017). Changes in regional heatwave characteristics as a function of increasing global temperature. *Scientific Reports*, *7*(1), 12256.

Philip, S. Y., Kew, S. F., van Oldenborgh, G. J., Anslow, F. S., Seneviratne, S. I., Vautard, R., ... Otto, F. E. L. (2021). Rapid attribution analysis of the extraordinary heatwave on the pacific coast of the us and canada june 2021. *Earth System Dynamics Discussions*, *2021*, 1–34. Retrieved from `https://esd.copernicus.org/preprints/esd-2021-90/` doi: 10.5194/esd-2021-90

Popovich, N., & Choi-Schagrin, W. (2021). Hidden toll of the northwest heat wave: Hundreds of extra deaths. *New York Times*.

Rex, D. F. (1950). Blocking action in the middle troposphere and its effect upon regional climate. *Tellus*, *2*(4), 275-301.

Risser, M., Collins, W., Wehner, M., O'Brien, T., Paciorek, C., O'Brien, J., ... Loring, B. (2022). A framework for detection and attribution of regional precipitation change: Application to the United States historical record. *Climate Dynamics*. doi: https://doi.org/10.21203/rs.3.rs-785460/v1

Risser, M., Wehner, M., O'Brien, J., Patricola, C., O'Brien, T., Collins, W., ... Huang, H. (2021). Quantifying the influence of natural climate variability

on in situ measurements of seasonal total and extreme daily precipitation. *Climate Dynamics*. doi: 10.1007/s00382-021-05638-7

Ruffault, J., Curt, T., Moron, V., Trigo, R. M., Mouillot, F., Koutsias, N., ... Belhadj-Khedher, C. (2020). Increased likelihood of heat-induced large wildfires in the mediterranean basin. *Scientific Reports*, *10*(1), 13790.

Schaller, N., Sillmann, J., Anstey, J., Fischer, E. M., Grams, C. M., & Russo, S. (2018). Influence of blocking on northern european and western russian heatwaves in large climate model ensembles. *Environmental Research Letters*, *13*(5).

Schär, C., Frei, C., Lüthi, D., & Davies, H. C. (1996). Surrogate climate-change scenarios for regional climate models. *Geophysical Research Letters*, *23*(6), 669-672.

Seneviratne, S. I., Zhang, X., Adnan, M., Badi, W., Dereczynski, C., Di Luca, A., ... Zhou, B. (2021). Weather and climate extreme events in a changing climate. in: Climate change 2021: The physical science basis. contribution of working group i to the sixth assessment report of the intergovernmental panel on climate change. Cambridge University Press.

Shutts, G. (2005). A kinetic energy backscatter algorithm for use in ensemble prediction systems. *Quarterly Journal of the Royal Meteorological Society*, *131*(612), 3079-3102.

Skamarock, W. C., Klemp, J. B., Dudhia, J., Gill, D. O., Barker, D. M., Duda, M. G., ... Powers, J. G. (2008). A description of the advanced research wrf version 3. *NCAR Technical Note NCAR/TN-475+STR.*.

Stone, D. A., Christidis, N., Folland, C., Perkins-Kirkpatrick, S., Perlwitz, J., Shiogama, H., ... Tadross, M. (2019). Experiment design of the International CLIVAR C20C+ Detection and Attribution project. *Weather and Climate Extremes*, *24*, 100206. doi: https://doi.org/10.1016/j.wace.2019.100206

Stott, P. A., Christidis, N., Otto, F. E. L., Sun, Y., Vanderlinden, J.-P., van Oldenborgh, G. J., ... Zwiers, F. W. (2016). Attribution of extreme weather and climate-related events. *WIREs Climate Change*, *7*(1), 23-41. Retrieved from `https://wires.onlinelibrary.wiley.com/doi/abs/10.1002/wcc.380` doi: https://doi.org/10.1002/wcc.380

Sumner, E. J. (1954). A study of blocking in the atlantic-european of the northern hemisphere. *Quarterly Journal of the Royal Meteorological Society*, *80*(345), 402-416.

Sun, Q., Miao, C., Hanel, M., Borthwick, A. G. L., Duan, Q., Ji, D., & Li, H. (2019). Global heat stress on health, wildfires, and agricultural crops under different levels of climate warming. *Environment International*, *128*, 125-136.

van Oldenborgh, G. J., van der Wiel, K., Kew, S., Philip, S., Otto, F., Vautard, R., ... van Aalst, M. (2021). Pathways and pitfalls in extreme event attribution. *Climatic Change*, *166*(1), 13. Retrieved from `https://doi.org/10.1007/s10584-021-03071-7` doi: 10.1007/s10584-021-03071-7

van Oldenborgh, G. J., Wehner, M. F., Vautard, R., Otto, F. E. L., Seneviratne, S. I., Stott, P. A., ... Kew, S. F. (2022). Attributing and projecting heatwaves is hard: we can do better. *Earth's Future*, *Submitted*.

Vogel, M. M., Zscheischler, J., Fischer, E. M., & Seneviratne, S. I. (2020). Development of future heatwaves for different hazard thresholds. *Journal of Geophysical Research: Atmospheres*, *125*(9), e2019JD032070. doi: https://doi.org/10.1029/2019JD032070

Wehner, M., Gleckler, P., & Lee, J. (2020). Characterization of long period return values of extreme daily temperature and precipitation in the CMIP6 models: Part 1, model evaluation. *Weather and Climate Extremes*, 100283. Retrieved from `http://www.sciencedirect.com/science/article/pii/S2212094719302440` doi: https://doi.org/10.1016/j.wace.2020.100283

Wehner, M., Stone, D., Shiogama, H., Wolski, P., Ciavarella, A., Christidis, N., &

Krishnan, H. (2018). Early 21st century anthropogenic changes in extremely hot days as simulated by the C20C+ detection and attribution multi-model ensemble. *Weather and Climate Extremes*, *20*, 1–8. Retrieved from `https://www.sciencedirect.com/science/article/pii/S2212094717301159` doi: https://doi.org/10.1016/j.wace.2018.03.001

Wehner, M., Zarzycki, C., & Patricola, C. (2019). Estimating the human influence on tropical cyclone intensity as the climate changes. In J. Collins & K. J. Walsh (Eds.), *Hurricane risk* (pp. 235–260). Springer.

Woollings, T., Barriopedro, D., Methven, J., Son, S.-W., Martius, O., Harvey, B., ... Seneviratne, S. (2018). Blocking and its response to climate change. *Current Climate Change Reports*, *4*(3), 287-300.

Wuebbles, D., Meehl, G., Hayhoe, K., Karl, T. R., Kunkel, K., Santer, B., ... Sun, L. (2014). Cmip5 climate model analyses: Climate extremes in the united states. *Bulletin of the American Meteorological Society*, *95*(4), 571-583.

Zhang, L., & Shaby, B. A. (2022). Reference priors for the generalized extreme value distribution. *Statistica Sinica*. doi: https://doi.org/10.5705/ss.202021.0258